Frequency Dependent Complex Refractive Indices of Supercooled Liquid Water and Ice Determined from Aerosol Extinction Spectra

A. Y. Zasetsky,* A. F. Khalizov, M. E. Earle, and J. J. Sloan

Department of Chemistry, University of Waterloo, Waterloo, Canada

Received: November 11, 2004; In Final Form: January 28, 2005

Complex refractive indices of supercooled liquid water at 240, 253, 263, and 273 K, and ice at 200, 210, and 235 K in the mid infrared from 460 to 4000 cm^{-1} are reported. The results were obtained from the extinction spectra of small (micron-size) aerosol particles, recorded using the cryogenic flow tube technique. An improved iterative procedure for retrieving complex refractive indices from extinction measurements is described. The refractive indices of ice determined in the present study are in good agreement with data reported earlier. The temperature region and range of states covered in the present work are relevant to the study of upper tropospheric and stratospheric aerosols and clouds.

Introduction

More than half of the total solar radiation incident upon Earth is absorbed by water, of which approximately 10^{16} kg is normally present in the atmosphere. A major portion of this water exists as vapor, making it the largest contributor to greenhouse warming of the atmosphere. The contribution of the condensed phases to radiative forcing is far less certain. Depending on the size of particles and their shape, water aerosol may contribute either to cooling, or warming, or to both. It is therefore essential to quantify the effects of these particles on the Earth's radiative balance. This, in turn, requires optical data for a variety of thermodynamic states over a wide range of temperatures.

Because of their great importance, the optical properties of liquid water and ice in the mid infrared at atmospheric pressure are well-documented.[1−6] Accurate data for the wavelength-dependent complex refractive indices of ice, $n^* = n + ik$, cover the temperature range between 100 and 266 K. For water, however, broad band mid infrared data are only available at room temperature, and there is a significant gap in the data at temperatures below 273 K. Supercooled liquid water droplets smaller than about 10 μm in diameter can exist for long times at temperatures down to about 238 K,[7] and it is the purpose of the present work to fill this gap in the temperature and wavelength dependent optical data. These conditions occur naturally in the lower stratosphere/upper troposphere, where supercooled water aerosol is observed in deep convective and cirrus clouds.[8]

Aerosol extinction spectroscopy has been used to determine optical constants since the pioneering works by Avery et al.[9] and Milham et al.[10] Later, the refractive indices of ice at lower temperatures were obtained using the extinction spectra of ice aerosol particles.[3] The starting point in both cases is "small particle spectra" − for which the scattering amplitude is negligible in the infrared, and hence the measured spectrum is a first approximation for the imaginary part of the refractive index k. Another way of obtaining an initial k spectrum is by the thin film technique.[11] Neither of these methods, however, is applicable to supercooled water. For thin film measurements, the interaction with the optical substrate changes the infrared absorption features significantly and also, the large volume due to the two macroscopic dimensions leads to early freezing, making deep supercooling of samples (below ~ 255 K) extremely difficult to achieve. In the case of the aerosol approach, it is very difficult to prepare samples of small (less than 0.3 μm) liquid water particles with high enough number density to provide reasonable signal-to-noise ratio. Due to the Kelvin effect and the rapid diffusion of water molecules, as well as collision induced coagulation, these small particles grow quickly to larger ones having diameters on the order of 1 μm. These have a significant scattering amplitude in the extinction spectrum. These difficulties have been overcome recently with the invention of a new method to correct the imaginary part of the refractive index, starting with approximate values as a first guess.[12] On the basis of this approach, we have developed an automated procedure for the determination of optical constants from extinction measurements of scattering aerosols.

Our motivation was to obtain a set of complex refractive indices for supercooled water, for use in our analysis of the liquid-to-crystal transition in water aerosols,[13] and also to provide more accurate data to the remote sensing and climate modeling communities. With this in mind, we calculated water and ice optical constants over a range of temperatures using the extinction spectra of small particles that were generated using the cryogenic flow tube technique.[13,14] In the present paper, we shall report the optical constants for ice and supercooled liquid water in the frequency range between 460 and 4000 cm^{-1}. An improved iterative procedure for retrieving complex refractive indices from extinction measurements is also reported.

Calculation Methodology

This section describes the iterative procedure for determining complex refractive indices from a set of IR extinction spectra, $I(\nu)$, and a first guess absorption spectrum, $k_0(\nu)$. The details of the algorithm are given in Appendix. Extinction spectra for this purpose can be computed using various techniques, such as Mie Theory,[15] T-matrix,[16] or Discrete Dipole[17,18] methods. Here we use the spherical approximation (Mie theory) and the Bohren and Huffman code[15] for ease of calculation, and because it is formally correct in the case of liquid particles. Although the ice particles are not spherical, they are small (less than 2 μm in diameter), so a spherical approximation is adequate for

10.1021/jp044823c CCC: $30.25 © 2005 American Chemical Society
Published on Web 03/08/2005

them as well. The initial guesses for the imaginary part of the refractive index, $k_0(\nu)$, have been taken from the data of Bertie and Lan[1] for water and of Warren[6] for ice.

The initial guess spectra, $k_0(\nu)$, were extended down to 0.1 cm^{-1} according to the following assumptions: first, we added the temperature-dependent librational mode at around 700 cm^{-1}, which is resolved in our experiment for ice and almost resolved for liquid supercooled water; second, we included the translational mode, which is assumed to have a weak temperature dependence due to its vibrational origin; and finally, we have added the dielectric relaxation mode in the microwave region with the temperature-dependent parameters taken from experimental studies[19] and our MD simulations.[13] With all of these modes included, and taking into account the fact that the spectrum of water has very weak absorption features from 4000 cm^{-1} up to 40000 cm^{-1}, we expect the Kramers−Kronig integral to be computed accurately.

Next, we address the problem of choosing values for the real part of the refractive index at infinite frequency—the so-called anchor points, n_∞, which are to be used in the subtractive Kramers−Kronig transform.[20,21] The n_∞ value for ice has been chosen to be the same as in ref 3. The anchor point values for water were taken from ref 22 (at 0.5145 μm) and ref 23 (at 0.5893 μm), where the refractive indices for water in the visible at temperatures as low as 263 and 268 K were reported. For the lower temperatures we use the extrapolated values. Comparison between these two sets of data has shown a negligibly small difference in the final results. For the purpose of the present study, we have chosen the following values for the anchor point at a wavelength of 0.5145 μm: 1.3350, 1.3363, 1.3368, and 1.3371 for water at 240, 253, 263, and 273 K, respectively.

The procedure, which follows the general approach given in ref 12 and 24, consists of two loops. The inner loop is a standard steepest descent iteration procedure, in which the imaginary part of the refractive index, $k(\nu)$, is scaled linearly through the variable k' (scaling coefficient). After each scaling, a Kramers−Kronig transform is performed on the adjusted $k(\nu)$ to produce a new set of optical constants $n^*(\nu)$. Then Mie calculations using the new optical constants are done to compute the extinction spectra for 96 discrete radii spanning the size range of the measured aerosol. The result is a new set of basis spectra (the matrix **K**, see ref 25 for detail) that are then used in the least-squares fitting of the measured spectrum, producing a new solution vector (size distribution) **P**. The technical details on solving the nonnegative least squares problem with constraints have been described in our earlier work.[25] These iterations are repeated while the increment Δk remains greater than ϵ_2 (in the present work this value was chosen to be 0.0005). In the outer loop, the values of $k(\nu)$ are corrected at each frequency according to the method proposed earlier.[12,24] The entire procedure is repeated until the difference between the norms at previous and current outer loop steps, $\chi^{previous} - \chi^{current}$, becomes less than ϵ_1. In the present work, we use the linear norm (1-norm), which is the sum of absolute differences between the experimental and computed extinction spectra. The convergence is reasonably fast—it requires 10−20 outer loop iterations to reduce the difference between previous and current norms ($\chi^{previous} - \chi^{current}$) to 0.05. The total number of iterations does not normally exceed 1000. The final values of the optical constants were computed by averaging the results for a set of experimental extinction spectra of aerosols with different size distributions. In the present case, the outcome ($n^*(\nu)$ values) of about 10 independent calculations for different particle size distributions have been used for each temperature.

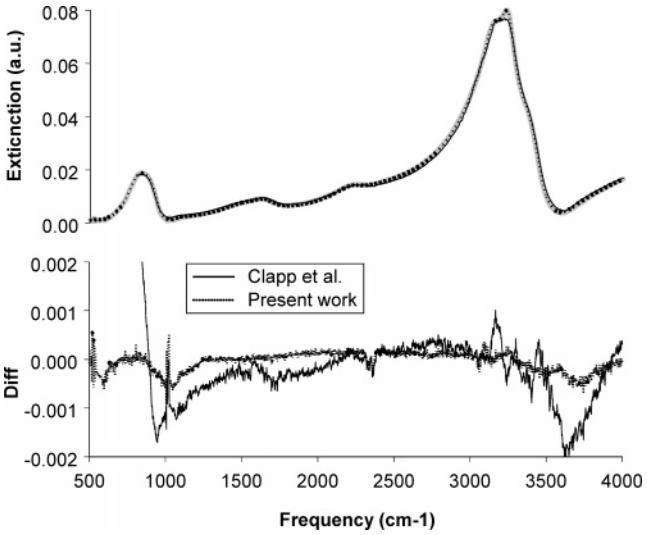

Figure 1. Extinction spectrum of ice aerosol at 200 K together with its best fits using the optical constants of Clapp et al. (solid line) and the results of the present work (dotted line). The differences between the fits and spectra are shown in the bottom plot.

We refer interested readers to refs 12 and 24 for the details of how the uncertainties in the refractive indices were estimated. In brief, the errors in the reported data arise from several sources, including detector and electronics noise (the signal-to-noise ratio was well above 10^4 across the frequency region employed), uncertainties in the minimization procedures, and error in the anchor point values. Taking into account all of these sources, we estimate that the uncertainties in both the real and imaginary part of the refractive index are frequency dependent and are largest (4%) in the O−H stretch region between 3100 and 3400 cm^{-1}. For the rest of the spectral region, the uncertainty in the real part is below 2%, and the uncertainty in the imaginary part is about 1.5%.

Experimental Details

The cryogenic flow tube technique was used to record the extinction spectra of liquid water and ice aerosols. A description of the apparatus and details of the experiment can be found elsewhere.[13,14] The flow tube has four independently coolable sections, each 38 cm long, with an inner diameter of 9 cm. The adjacent sections are connected by thin-walled stainless steel bellows that allow each section to be maintained at a different temperature. The entire assembly is enclosed in an evacuated stainless steel jacket to provide thermal isolation. The temperature deviations along a section are within ±0.5 K. Externally generated particles and water vapor were introduced in a nitrogen flow (0.5−3.0 SLPM) through a heated inlet at the top of the flow tube, where they were mixed with pre-cooled nitrogen carrier gas (7−10 SLPM). Water droplets with median sizes of 2.0 and 4.0 μm were produced by a constant output atomizer (TSI 3076, TSI Inc.) and by an ultrasonic nebulizer (UltaNeb 99, De Vilbiss Co.), respectively. The smallest particles, at about 1.0 μm, were generated by heterogeneous condensation of water vapor on 5 nm sodium chloride particles. A series of additional experiments (not reported here) showed that NaCl at this very low concentration (10^{-4} M) affects neither optical nor freezing properties of water aerosol.

After conditioning in the first section at 283 K, aerosol was cooled in the subsequent sections to the desired temperature

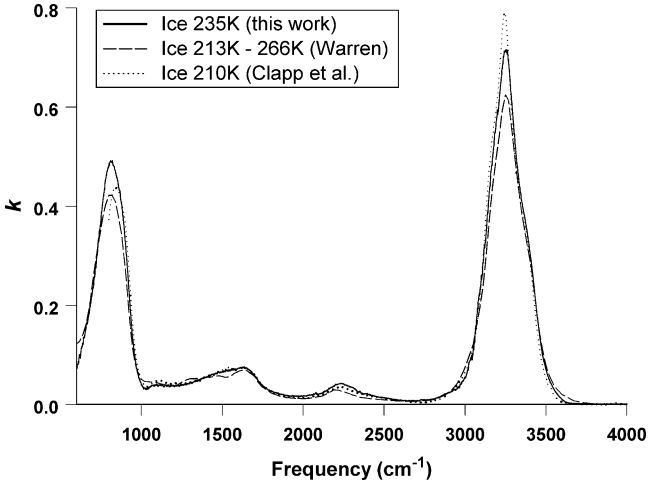

Figure 2. Comparison between the imaginary parts of the refractive indices of ice at different temperatures. The result of the present work (235 K) is shown by solid lines, Warren (266 K) and Clapp et al. (210 K) data are shown by dashed and dotted lines, respectively.

(230−278 K). Infrared spectra were recorded by passing a collimated IR beam, modulated by a Michelson interferometer (Bruker Tensor 37), through the optical ports in the bottom section. After passing across the aerosol flow, the beam was focused by an off-axis parabolic mirror onto an MCT detector (FTIR-22-1.0, Infrared Associates). Each spectrum is an average of 80 scans collected in the frequency range from 450 to 6000 cm^{-1}, at 1 cm^{-1} resolution and 40 kHz metrology frequency. Water vapor spectra recorded at the same temperatures were subtracted from the measured aerosol extinction spectra.

Results and Discussion

We report the complex refractive indices of supercooled water and ice in an extended frequency range from 460 to 4000 cm^{-1} and compare these with previous studies. To assess the accuracy of our procedure, we calculated the refractive indices of ice at 200 K for which previous accurate measurements exist.[3] Figure 1 shows an extinction spectrum of ice aerosol at 200 K that has been fitted using the frequency dependent complex refractive indices of ice determined by us and by Clapp et al.[3] The residuals from the two fits are also shown. Good agreement is evident from about 1500 to 3100 cm^{-1}. The divergence in the region below 1500 cm^{-1} is likely due to errors associated with the contribution from the low-frequency absorption modes to the Kramers−Kronig integration. A noticeable improvement in the Mie fits indicates that our data are quite accurate in this low-frequency region. There are still some discrepancies in the O−H stretching region where uncertainties are the largest due to very strong absorption, but the deviations are not dramatic (<2%).

One of the aims of the present work was to obtain the optical constants of ice at a temperature close to the freezing point of micron-sized supercooled water aerosols (roughly around 235 K). We require this to obtain a quantitative measurement of the phases present during the freezing transition.[13] The temperature dependence of the optical constants is significant in this region, as demonstrated in Figure 2, which shows the imaginary part of the refractive indices of ice determined at 235 K in comparison with the data of Clapp et al.[3] (210 K) and Warren[6] (compiled from the data measured in the temperature range from 213 to 266 K). The differences between these data sets are primarily due to the temperature dependence of the optical constants, except for the frequency region below 1500 cm^{-1}, in which we believe our data are more accurate due to proper accounting for the low-frequency region in the Kramers−Kronig integration.

The extinction spectra of water at 240 K together with their best Mie fits are shown in Figure 3. The fits are calculated using the optical constants derived by the procedure described in the present paper and our earlier publication.[25] Excellent agreement between the experimental and computed extinction spectra is evident in all cases. As can be seen from volume size distributions corresponding to these fits, we can vary the particle size in the range between 0.5 and 5 μm using different experimental techniques to generate particles.[13] We note that more stable solutions are achieved by using the spectra of smaller (0.5 $\mu m < r < 2.0\ \mu$m) particles; a plausible explanation of this fact is that the spectra of small particles are less distorted by scattering and, therefore, provide more accurate retrieval

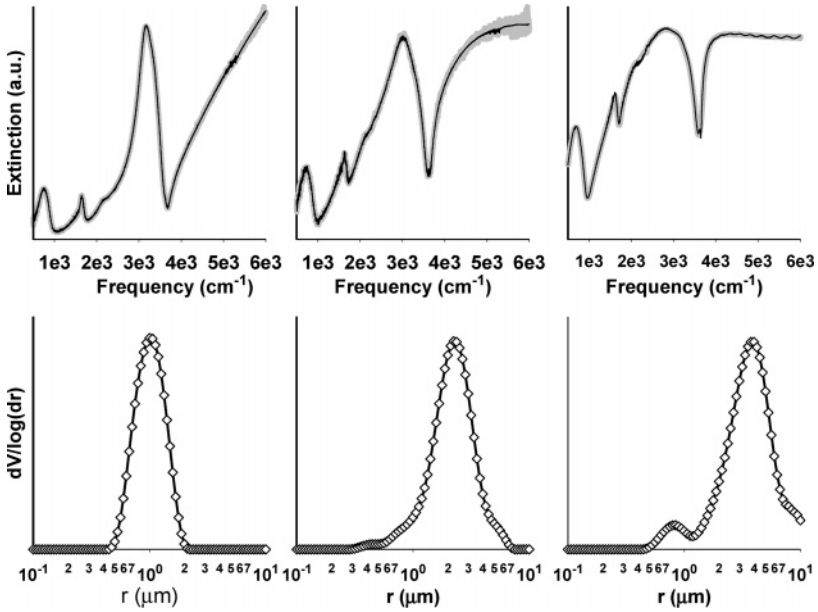

Figure 3. Experimental extinction spectra of water aerosols (thick gray lines) together with their best fits (solid black lines) at 240 K. Corresponding volume size distributions are shown below for each spectrum.

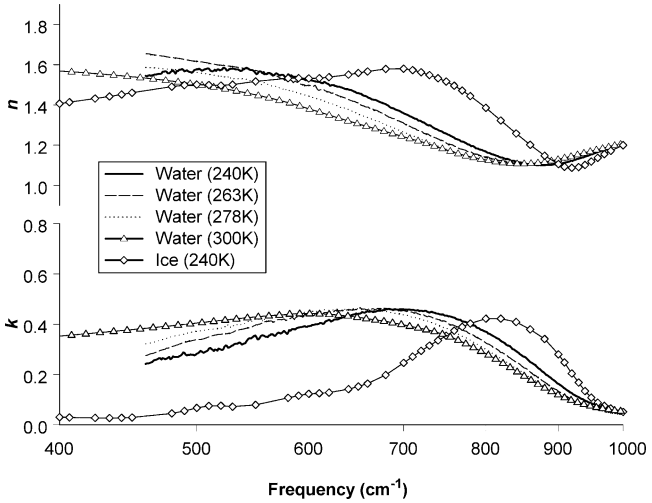

Figure 4. Temperature-dependent refractive indices for liquid water determined in the present study: solid (240 K), dashed (263 K), and dotted (273 K) lines in comparison with those of Bertie (298 K, triangles) and the refractive indices of ice (Warren) in the frequency range from 450 and 1000 cm^{-1}.

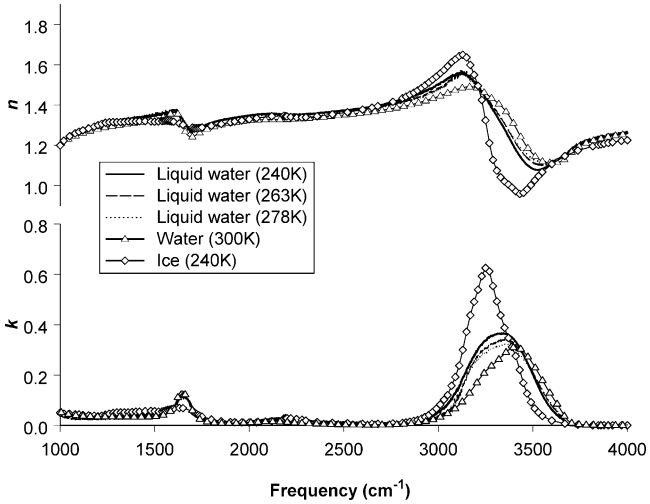

Figure 5. Same as in Figure 4 for the frequency range from 1000 and 4000 cm^{-1}.

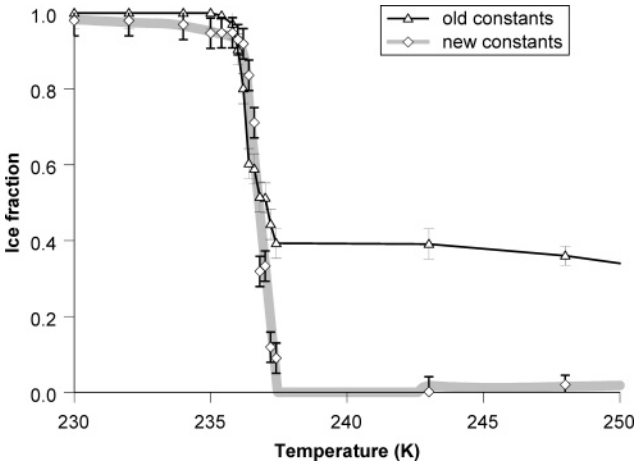

Figure 6. Freezing transition in micron-size aerosols. The use of the refraction indices of supercooled water makes possible an accurate description of the liquid-to-crystal transition in water aerosol. "Old" constants were taken from Warren[6] for ice and from Bertie and Lan[1] for water. "New" constants are determined in the present work.

results. The broad particle size range used here allows us to overcome the issue of nonuniqueness of the particle size distribution. This problem was raised previously,[3] where the authors noted that the use of particles larger than 0.5 μm may "guarantee uniqueness" of the size distribution.

There is a very large uncertainty in the freezing nucleation rate constant,[26−29] so it is necessary to establish that the particles in Figure 3, for which we have derived optical constants, are indeed *liquid*. If we assume an upper limit of 100 cm^{-3} s^{-1} for the ice nucleation rate constant at 240 K, which is an order of magnitude greater than the generally accepted value,[28] then 10 μm droplets, which are at least twice as large as we observed in our experiments, would require 10^5 to 10^6 s to freeze. The average residence time in the flow tube is less than 10^2 s. Thus, we can safely state that the particles we observe at 240 K are composed of liquid water. Moreover, when nucleation of ice does occur, we observe that it is followed immediately by extensive mass transfer of water vapor from the remaining liquid droplets to the nascent ice crystals, leading to a significant increase in scattering above 4000 cm^{-1} in the infrared spectra. We did not observe such changes in scattering in these experiments.

Figures 4 and 5 show the refractive indices determined in the present study; data for water at room temperature and ice at 240 K are also presented for comparison. The refractive indices of liquid water show significant temperature dependence over the temperature range between 273 and 240 K. In the lower frequency region (see Figure 4), the librational mode, which is centered at 600 cm^{-1} for liquid water at room temperature, shifts toward higher frequencies, and reaches 700 cm^{-1} for deeply supercooled liquid water and 800 cm^{-1} for ice. Therefore, we would like to stress, once again, that the addition of the temperature-dependent translational, librational, and dielectric relaxation modes to the Kramers−Kronig integration is critical to improving the accuracy of the data for frequencies less than about 1500 cm^{-1}. (The accuracy in the vicinity of the librational mode was reported to be a problem in the previous studies of ice[3].)

The refractive indices in the O−H stretching region also show significant temperature dependence. The main peak shifts toward lower frequencies: from 3400 cm^{-1} for water at room temperature to 3330 cm^{-1} for supercooled water at 240 K. These features shift smoothly and continuously toward the corresponding ice refractive indices, which are shown for comparison, suggesting that supercooled water acquires "ice-like" character.[13] This smooth shift makes it difficult to describe the freezing transition in water aerosol. Using the new refractive indices for liquid supercooled water and ice over the temperature range from 237 to 235 K, however, we now can determine this freezing transition in liquid water aerosols quite accurately. Recording the spectra of the aerosols as a function of temperature in the cryogenic flowtube, and using the retrieval procedure described previously,[25] we obtain the results shown in Figure 6. The two curves are the results of analyzing the same measured data using the two sets of optical constants. Because of the smooth transition in the optical properties of water with temperature, noted above, the use of the previously available optical constants for water at 298 K leads to erroneous retrieval of a significant fraction of ice in the liquid droplets. The refractive indices obtained in the present study enable a much more accurate description of this freezing transition, permitting the quantification of supercooled water and ice from infrared measurements. This has applications in atmospheric remote sensing as well as in laboratory measurements. Because water, supercooled water and ice aerosols all have different radiative characteristics, the accurate quantification of all three in the

atmosphere—using infrared satellite remote sensing, for example—will greatly improve our ability to calculate their effects on radiative forcing.

Acknowledgment. We are grateful for the financial support of the Natural Sciences and Engineering Research Council of Canada. We thank Professor Richard Niedziela for encouragement and valuable discussions.

Supporting Information Available: The refractive indices of supercooled water and ice. This material is available free of charge via the Internet at http://pubs.acs.org.

Appendix

The present iterative procedure is based on algorithms that have been successfully applied to aerosol extinction spectra to obtain complex refractive indices of various materials.[3,11,12] The general algorithm used in the present study is given below

do while ($\chi^{previous} - \chi^{current} > \epsilon_1$)

$\Delta k = \Delta k_0$

do while ($\Delta k > \epsilon_2$)

$k(\nu) = k' k_0(\nu)$, $k' = 1 + \Delta k$

!scale absorption coefficient

$$n(\tilde{\nu}_i) = n_\infty + \frac{2L}{\pi}\int_0^\infty \frac{\tilde{\nu} k(\tilde{\nu})}{\nu_i^2 - \tilde{\nu}^2} d\tilde{\nu};\ i=1,N^{ext}$$

!perform KK transform

$Q_{j,i}^{ext,scatt}[n^*(\nu_i), r_j]$; $i = 1,N$, $j = 1,M$

!compute extinction efficiency (Mie)

$K_{j,i}^V = 3Q_{j,i}^{ext}/2r_j$; $i = 1,N$, $j = 1,M$

!normalize to the particle volume

$$\min_{\mathbf{P}}\{ |\mathbf{K}^V \cdot \mathbf{P} - \mathbf{I} + \gamma \cdot \mathbf{S} \cdot \mathbf{P}|^2 \}^{1/2}, \text{ subject to } \mathbf{1} \cdot \mathbf{P} \geq \mathbf{0}$$

!solve linear system

$\chi^{current} = |\mathbf{K}^V \cdot \mathbf{P} - \mathbf{I}|$!compute 1-norm

if($\chi^{current} > \chi^{previous}$) $\Delta k = -\Delta k/2$

end do while !(ϵ_2)

for $i = 1,N$

$$\Delta I_i = I(\nu_i) - \sum_{j=1}^{M} K_{j,i}^V \cdot P_j;$$

$$\tilde{Q}_i^{ext} = \sum_{j=1}^{M} Q_{i,j}^{ext} \cdot P_j;$$

$$\tilde{Q}_i^{scat} = \sum_{j=1}^{M} Q_{i,j}^{scat} \cdot P_j;$$

$$k(\nu_i) = k(\nu_i) + \frac{\Delta I_i}{\nu_i}(1 - \tilde{Q}_i^{scat}/\tilde{Q}_i^{ext})$$

!correct imaginary part of refractive index

end for

end do while !(ϵ_1)

In the above equations: $K_{j,i}^V$ is the aerosol extinction cross section at the frequency ν_i, normalized to the volume of a sphere with radius r_j; Q^{ext} and Q^{scat} are the extinction and scattering efficiency coefficients, respectively; $n^*(\nu) = n(\nu) + ik(\nu)$ is the complex refractive index; r is the particle radius; and ν is the frequency. The vector **I** is the (observed) extinction spectrum and **1** is the identity matrix. The description of the matrix **S** can be found in ref 25. The solution vector **P** gives the volume size distribution after normalization by the total volume of aerosol particles. The matrix **K** is an $N \times M$ matrix column, in which N is the number of frequencies (~4000), M is the number of discrete radii, and N^{ext} is the number of points used in the discrete Kramers−Kronig integration, which is different from N as an extended frequency range is used. The n_∞ quantity is the refractive index at infinite frequency, k' is the scaling coefficient, and χ is the norm. The quantities ϵ_1 and ϵ_2 are small numbers that are used to specify the stop criteria for the outer and inner loop, respectively.

References and Notes

(1) Bertie, J. E.; Lan, Z. D. *Appl. Spectrosc.* **1996**, *50*, 1047−1057.
(2) Buch, V.; Devlin, J. P. *J. Chem. Phys.* **1999**, *110*, 3437−3443.
(3) Clapp, M. L.; Miller, R. E.; Worsnop, D. R. *J. Phys. Chem.* **1995**, *99*, 6317−6326.
(4) Devlin, J. P.; Joyce, C.; Buch, V. *J. Phys. Chem. A* **2000**, *104*, 1974−1977.
(5) Toon, O. B.; Tolbert, M. A.; Koehler, B. G.; Middlebrook, A. M.; Jordan, J. *J. Geophys. Res.−Atmos.* **1994**, *99*, 25631−25654.
(6) Warren, S. G. *Appl. Opt.* **1984**, *23*, 1206−1225.
(7) Debenedetti, P. G. *J. Phys.−Condens. Matter* **2003**, *15*, R1669−R1726.
(8) Sassen, K. *Science* **1992**, *257*, 516−519.
(9) Avery, R. K.; Jones, A. R. *J. Phys. D−Appl. Phys.* **1982**, *15*, 1373−1384.
(10) Milham, M. E.; Frickel, R. H.; Embury, J. F.; Anderson, D. H. *J. Opt. Soc. Am.* **1981**, *71*, 1099−1106.
(11) Sutherland, R. A.; Khanna, R. K.; Ospina, M. J. *Aerosol Sci. Technol.* **1994**, *20*, 62−70.
(12) Dohm, M. T.; Potscavage, A. M.; Niedziela, R. F. *J. Phys. Chem. A* **2004**, *108*, 5365−5376.
(13) Zasetsky, A. Y.; Khalizov, A.; Sloan, J. J. *J. Chem. Phys.* **2004**, *14*.
(14) Bertram, A. K.; Sloan, J. J. *J. Geophys. Res.−Atmos.* **1998**, *103*, 3553−3561.
(15) Bohren, G.; Huffman, D. *Absorption and Scattering of Light by Small Particles*; Wiley: New York, 1983.
(16) Mishchenko, M. I.; Travis, L. D. *J. Quant. Spectrosc. Radiat. Transfer* **1998**, *60*, 309−324.
(17) Draine, B. T.; Flatau, P. J. *J. Opt. Soc. Am. A* **1994**, *11*, 1491−1499.
(18) Draine, B. T.; Flatau, P. J. *Astrophys. -ph/0309069*, http://arxiv.org/abs/astro-ph/0309069.
(19) Ronne, C.; Keiding, S. R. *J. Mol. Liq.* **2002**, *101*, 199−218.
(20) Hawranek, J. P.; Neelakantan, P.; Young, R. P.; Jones, R. N. *Spectrochim. Acta* **1976**, *32A*, 85−98.
(21) Ohta, K.; Ishida, H. *Appl. Spectrosc.* **1988**, *42*, 952−957.
(22) Harvey, A. H.; Gallagher, J. S.; Sengers, J. M. H. L. *J. Phys. Chem. Ref. Data* **1998**, *27*, 761−774.
(23) Robinson, G. W.; Cho, C. H.; Gellene, G. I. *J. Phys. Chem. B* **2000**, *104*, 7179−7182.
(24) Clapp, M. L.; Niedziela, R. F.; Richwine, L. J.; Dransfield, T.; Miller, R. E.; Worsnop, D. R. *J. Geophys. Res.−Atmos.* **1997**, *102*, 8899−8907.
(25) Zasetsky, A. Y.; Khalizov, A.; Sloan, J. J. *Appl. Opt.* **2004**, *43*, 5503−5511.
(26) Demott, P. J.; Rogers, D. C. *J. Atmos. Sci.* **1990**, *47*, 1056−1064.
(27) Kramer, B.; Hubner, O.; Vortisch, H.; Woste, L.; Leisner, T.; Schwell, M.; Ruhl, E.; Baumgartel, H. *J. Chem. Phys.* **1999**, *111*, 6521−6527.
(28) Pruppacher, H. R.; Klett, J. D. *Microphysics of Clouds and Precipitation*; Kluwer Academic Publishers: London, 1998.
(29) Stockel, P.; Vortisch, H.; Leisner, T.; Baumgartel, H. *J. Mol. Liq.* **2002**, *96−7*, 153−175.